Flower-like Photonic Hydrogel with Superstructure Induced via Gradient Shear Field

Journal:	*ACS Macro Letters*
Manuscript ID	mz-2021-00178j
Manuscript Type:	Letter
Date Submitted by the Author:	17-Mar-2021
Complete List of Authors:	YE , YA NAN ; Hokkaido University Haque, Md; Dhaka University, Department of Chemistry Inoue, Akane ; Hokkaido University Katsuyama, Yoshinori; Hokkaido University Kurokawa, Takayuki; Hokkaido University, Gong, Jian Ping; Hokkaido University , Faculty of Advanced Life Science

Flower-like Photonic Hydrogel with Superstructure Induced via Gradient Shear Field

Ya Nan Ye[1#], M. Anamul Haque[2,3#], Akane Inoue[4], Yoshinori Katsuyama[2] Takayuki Kurokawa[1,2] and Jian Ping Gong[1,2,5*]*

[1]Global Institution for Collaborative Research and Education (GI-CoRE), Hokkaido University, Sapporo 001-0021 Japan;

[2]Faculty of Advanced Life Science, Hokkaido University, Sapporo 001-0021, Japan;

[3]Department of Chemistry, University of Dhaka, Dhaka 1000, Bangladesh;

[4]Graduate School of Life Science, Hokkaido University, Sapporo 001-0021 Japan;

[5]Institute for Chemical Reaction Design and Discovery (WPI-ICReDD), Hokkaido University, Sapporo 001-0021 Japan.

* Kurokawa Takayuki

Email: kurokawa@sci.hokudai.ac.jp

* Jian Ping Gong

Email:gong@sci.hokudai.ac.jp

[#]These authors contributed equally to this work.

Abstract Biological tissues usually have complex superstructures and elaborated functionalities. However, creating superstructures in soft and wet hydrogels is challenging because of the absence of effective approaches to control the molecular orientation. Here we introduce a method to create superstructures in photonic hydrogels comprised of lamellar bilayers intercalated in the crosslinked polymer network. The orientation of lamellar bilayers in the photonic gel, which are sensitive to

shear stress field, is modulated by applying a gradient shear field on the precursor solution using a customized rheometer. The difference in orientation of lamellar bilayers leads to swelling mismatch in the radial direction, endowing the disk-shape hydrogel with a macroscopic flower-like shape with a central dome and an edge petal, along with a bright photonic color. By characterizing the swelling anisotropy of radial profile, the shear rate required for the uniaxial orientation of lamellar bilayers was extracted. Moreover, a delayed polymerization experiment was designed to measure the lifetime of aligned lamellar bilayers, which reveals the domain size of lamellar bilayers in the precursor solution. Furthermore, we also demonstrated that the hydrogel flowers could fade and rebloom reversibly in response to external stimuli. This work presents a novel strategy to develop gradient superstructures in hydrogels and sheds light on designing biomimetic materials with intricately architectural gradient.

Keywords: Photonic hydrogel, superstructure, gradient shear field, flower-like, lamellar bilayer

Introduction Hydrogels are soft and water-containing materials.[1–4] They received ever-increasing attention as promising regenerative biomaterials due to their similarity to biological tissues.[5,6] While many biological tissues, such as muscle, tooth or bone, exhibit hierarchical structures from macroscopic to microscopic length scales, endowing them with unique biological functionalities.[7–9] Taking the bone as an example, the macroscale arrangements involve lamellar compact/cortical part at the surface and isotropic spongy/trabecular part in the interior with a radially

intricate gradient.[10] Such natural materials are built through bottom-up strategies[11], which are difficult to duplicate in large-scale manufacturing of human-engineered materials.[12,13] Introducing macroscale superstructures into isotropic and amorphous hydrogels to mimic the features of natural materials remains a big challenge.

Herein, we report a facile method to develop hydrogels with superstructure from molecular to macroscopic level from dodecyl glyceryl itaconate (DGI) monomers and acrylamide (AAm) monomers. Dodecyl glyceryl itaconate (DGI) monomers can self-assemble into bilayers, and the bilayers periodically stack into microscopic lamellar domains in the precursor solution.[14] After polymerization, the lamellar structure was immobilized inside the PAAm network by the hydrogen bonding between hydroxyl group in DGI and amide group in PAAm. Without imposing shear flow, the lamellar domains are randomly orientated in the precursor solution. When a shear flow was imposed, the lamellar domains were oriented along the shear direction to form macroscopic lamellar domains with unidirectional alignment in the precursor solution. After polymerization, the gels without applying a shear have an isotropic structure in macroscopic scale, showing isotropic properties such as swelling.[15,16] On the contrary, gels with sufficient shear is anisotropic, showing perfect one-dimensional swelling in the direction perpendicular to the lamellar bilayers while the swelling along the bilayers are completely suppressed due to the water-impermeable nature of the rigid PDGI bilayers.[17]

In this work, we take advantage of the high sensitivity of the lamellar domain orientation to the shear flow imposed on the precursor solution and

construct multiscale superstructure in the hydrogels. We customized a device capable of imposing gradient shear flow and conducting UV polymerization after shear. The gradient shear flow is realized through rotational movement of two coaxial parallel disk plates with different radius. For the precursor solution between two plates, the shear rate varies from zero to maximum along the radial direction, while the precursor solution outside the smaller plate does not suffer shear flow. Through such a modulated flow field, lamellar domains with different degree of orientation can be obtained in one piece of gel. Such superstructure leads to a swelling mismatch in the gel to show a flower-like shape, with a central dome and an edge petal. The shape of the gel flower can be controlled through tuning shear field, polymerization temperature, and the duration between shear and polymerization. The gel flower can fade and rebloom reversibly to response to external stimuli.

Results and discussion

Superstructure formation in photonic hydrogels. In the precursor solution, the DGI monomers can self-assemble into bilayer domains without a preferred orientation (Figure 1a). After being loaded between two coaxially parallel disk plates of a customized rheometer, a shear flow was imposed by the rotation of the upper plate while the lower plate was fixed (Figure S1). In this way, a gradient shear flow field with the shear rate of $\dot{\gamma} = \omega r/t$ from center to edge was built.[18] Here ω, r, and t are the angular speed of rotation, the radial distance from the center of the plates, and the gap distance between two plates, respectively (Figure 1b).

Due to the high sensitivity to the shear flow, a gradient-increased orientation degree of lamellar domain from center to edge was achieved. The upper plate radius is 17.5 mm, which is smaller than that of the lower plate (20 mm). In the region between the edges of the upper and lower plates, the shear flow is negligible, resulting in randomly dispersed bilayer domains. After the cessation of shear flow, the above superstructure was immobilized inside the PAAm network by concurrent homopolymerization through an ultraviolet (UV) polymerization system (Figure S1 and Figure 1c). This is realized by using a glass plate as the lower plate, which is transparent and allows the penetration of UV light.

The as-prepared gels were transparent. After immersing in water, the gels show bright structural color and a macroscopic flower shape (Figure 1d). The macroscopic hydrogel flower consists of three parts: a small dome in central region, a plate shape in the middle region, and a petal in the edge region. Such a macroscopic hydrogel flower was formed due to the swelling mismatch of different parts of the gel. In the central point and the region between the edge of the two plates, the shear rate is zero and the rigid PDGI bilayers have no preferred orientation. These parts of gel show isotropic swelling. While in the region between them, the orientation of PDGI bilayers gradually increases with the distance from center because of the increase of the shear rate $\dot{\gamma}$.[19] Above a certain $\dot{\gamma}$, the PDGI bialyers show an unidirectional alignment, and the gel only shows 1D swelling in the sample thickness direction, which is perpendicular to the lamellar bilayers. The swelling mismatch between different regions induces internal stress in the hydrogel, which directs the formation of macroscopic hydrogel

flower. The structural color is from lamellar structure comprised of periodical stacking of PDGI bilayers and PAAm hydrogel layers.

For simplicity, we called the region sandwiched by the parallel plates as the main region and the region out of sandwiched plates as the petal region. The color in the main region can be tuned by adjusting the polymerization temperature (**Figure S2**), DGI concentration[17] and AAm concentration[20], etc.

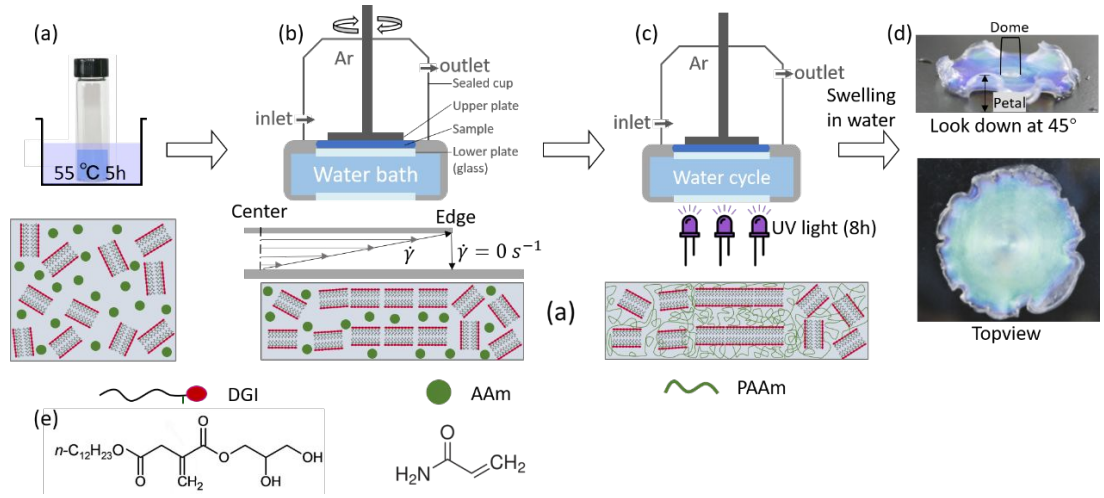

Figure 1. Schematic diagram depicting the preparation of a photonic hydrogel flower. (a) The precursor solution was kept in a temperature-controlled water bath to dissolve the DGI monomer into bilayer domains. (b) Then the precursor solution was loaded between the parallel plates with a gap distance of 0.5 mm of a customized rheometer and followed by applying a gradient shear between two parallel plates, which increases from 0 to $\omega R/t$ from center to edge. Where ω, R and t are the angular speed of rotation, upper plate radius, and gap distance between upper and lower plates, respectively. As a result, the orientation degree of the DGI bilayers increased from center to edge. In addition, the precursor solution out of the sandwiched plates has negligible orientation. (c) Finally, those superstructures were fixed by a concurrent homopolymerization of DGI and AAm using UV light irradiation from the lower plate side to form gels. The gel was immersed in water for 1 week for equilibrium. The mismatch of the swelling from center to edge is the main driving force of the photonic flower formation (d). (e) Main chemicals used in this work.

Evidence for the formation of gradient orientated structure between the upper and lower plates. To confirm the formation of gradient structure between the upper and lower plates caused by the gradient shear rate, polarizing microscopic images (POM) on the region between the upper and lower plates were taken from the cross-section of the gel sample (Figure 2a,b). The gel piece near the central point shows weak and heterogeneous birefringence, indicating the relatively random orientation of lamellar domains (position 3 in photo of Figure 2a). On the contrary, the gel piece far from the central point of the gel shows strong and homogeneous birefringence, indicating a uniform in-plane orientation of lamellar domain (position 1 in photo of Figure 2a).

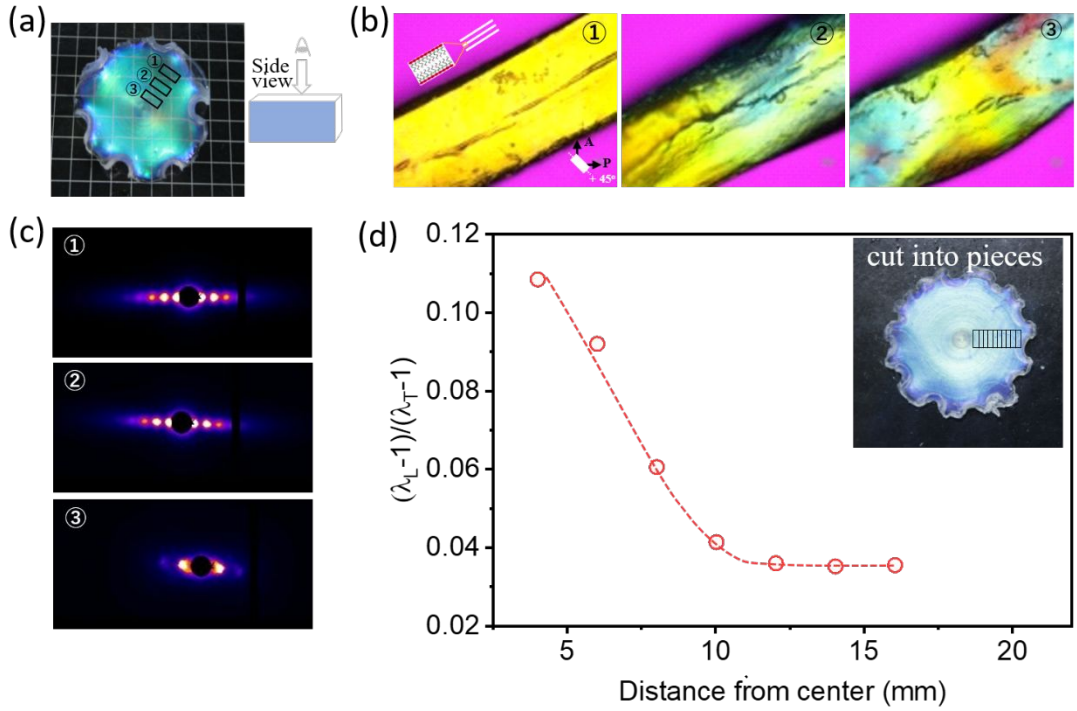

Figure 2. Characterization of the gradient structure of the photonic hydrogel flowers. (a) The optical images of the sample and the three representative positions for structure characterization by POM and SAXS from the sideview. (b) POM images with 530 nm sensitive tint plate

measured at different distances from the centers as shown in (a). (c) 2D small angle X-ray scattering images captured at different distances from the centers as shown in (a). (d) Position dependence of anisotropy parameters $(\lambda_L - 1)/(\lambda_T - 1)$, where λ_L and λ_T are size ratios in water to that in 10 wt.% (polyethylene glycol) PEG solution for the directions parallel to and perpendicular to the sample sheet, respectively. For an isotropic swelling, $(\lambda_L - 1)/(\lambda_T - 1) = 1$, while for a one-dimensional swelling of uniaxially aligned lamellar domain, $(\lambda_L - 1)/(\lambda_T - 1) = 0$.

The formation of gradient structure between the two plates was further verified by small-angle X-ray scattering (SAXS) experiment. SAXS images at different positions of the gel from the side view exhibit different scattering features. The position 1 in Figure 2a that far from the central point show anisotropic scattering patterns with symmetric pots up to the fourth order (Figure 2c). Such symmetric spots originated from the highly orientated periodic 1D lamellar structure.[21] While the anisotropic scattering patterns become broaden along the azimuthal direction, and the scattering spots decrease to the second order for the position 1 that near the central point of the gel, suggesting that the orientation and periodicity of the lamellar structure become worse at low shear rate. The 2D SAXS patterns were integrated into 1D SAXS curves to extract the *d*-spacing of lamellar structure (Figure S3). The *d*-spacing at different positions are almost the same of about 310 nm, which is responsible for the bright structural color of the gel. This also suggests that the shear flow mainly determines the orientation of the lamellar structure but has negligible influence on the *d*-spacing.

The anisotropy of the gradient structure formed between the two plates was further quantified by using an osmotic stress method. For PDGI/PAAm hydrogels with unidirectional alignment of lamellar bilayer, it shows perfect one-dimensional swelling in pure water in the direction perpendicular to the lamellar bilayers. On the contrary, the PDGI/PAAm hydrogels without preferred orientation of lamellar bilayer show isotropic swelling in water.[17] Accordingly, the water-swollen samples will shrink in high osmotic solution, and the shrinking anisotropy reveals the structure anisotropy. We first confirmed the shrinking behavior of a water-swollen PDGI/PAAm hydrogel with homogeneous unidirectional alignment of lamellar bilayer in polyethylene glycol (PEG) solution (Figure S4). The gel gradually decreased its thickness with the increase of PEG concentration, while the lateral size of the gel did not change. The size ratios in water and PEG solution were calculated as $\lambda_L = \frac{L_0}{L_1}$ for lateral direction and $\lambda_T = \frac{T_0}{T_1}$ for thickness direction of the sample. Where the L_0 and T_0 are the length and thickness equilibrated in water, respectively; The L_1 and T_1 are the length and thickness equilibrated in PEG solution, respectively. Here we define an anisotropy parameter, $(\lambda_L - 1)/(\lambda_T - 1)$. For the isotropic structure, the gel swells (in water) or shrinks (PEG solution) isotopically (λ_L=λ_T), so $(\lambda_L - 1)/(\lambda_T - 1) = 1$; For the PDGI/PAAm gel with unidirectional alignment of lamellar bilayer, the lateral direction of the gel does not swell or shrink $(\lambda_L = 1)$, which gives $(\lambda_L - 1)/(\lambda_T - 1) = 0$.

Next, we cut the gel formed under gradient shear into small pieces along the radial direction (Inserts of Figure 2d) and immersed these specimens into a 10 wt.% PEG aqueous solution. Figure 2d shows the change of $(\lambda_L - 1)/(\lambda_T - 1)$ with increasing the distance from the central point of a gel with ω of 11.4 s^{-1}. The $(\lambda_L - 1)/(\lambda_T - 1)$ decreases quickly with increasing the distance from center point of the gel, suggesting a gradual increase of the alignment of lamellar bilayer with increasing shear rate. $(\lambda_L - 1)/(\lambda_T - 1)$ reaches a plateau of about 0.03 for the sample with a distance larger than 10 mm, suggesting the formation of unidirectional alignment of lamellar bilayer at a shear rate larger than a critical value. This critical shear rate can be calculated with the relation $\omega r/t$, which is around 200 s^{-1}. The swelling result also shows that even at a position quite close to the center, the gel still shows certain anisotropy, consistent with the results obtained by POM and SAXS.

Tunable superstructure by shear rate. The superstructure of the hydrogels can be well-controlled by tuning the shear rates. **Figure 3a** shows the optical pictures of the photonic gels prepared by different angular speeds ω ranging from 11.4 to 42.9 rad/s. As shown in **Figure 3b**, the radius of dome, r^*, decreases as increasing ω. Specifically, the radius of dome is 2.0 mm for a ω of 11.4 rad/s, while it decreases to about 0.5 mm for ω of 42.9 rad/s. The shear rate at the edge of dome can be estimated by the relation $\dot{\gamma}^* = \omega r^*/t$, which hardly depended on ω (**Figure 3c**). The almost constant $\dot{\gamma}^*$ of 60 s^{-1} suggests that the formation of dome depends on the shear rate, which controls the alignment of lamellar

bilayers and consequent swelling mismatch. The anisotropy parameter $(\lambda_L - 1)/(\lambda_T - 1)$ of gels at different ω were measured and plotted as a function of $\dot{\gamma}$. As shown in **Figure 3d**, all the anisotropy parameters for the gels prepared at ω ranging from 1.4 to 42.9 s^{-1} were collapsed into one master curve. This further confirmed that the alignment of lamellar bilayers in hydrogels, which causes the swelling mismatch, depends on the shear rate imposed on the precursor solution. The $(\lambda_L - 1)/(\lambda_T - 1)$ first decreases with shear rate and then reaches a plateau around 200 s^{-1}, suggesting that the perfect alignment of lamellar bilayers happens at the shear rate larger than 200 s^{-1}. This shear rate is much larger than $\dot{\gamma}^*$ for dome formation (60 s^{-1}), suggesting the dramatic swelling mismatch happens at a shear rate of 60 s^{-1}. Indeed, the anisotropy parameter, $(\lambda_L - 1)/(\lambda_T - 1)$, changes dramatically at the shear rate of 60 s^{-1}.

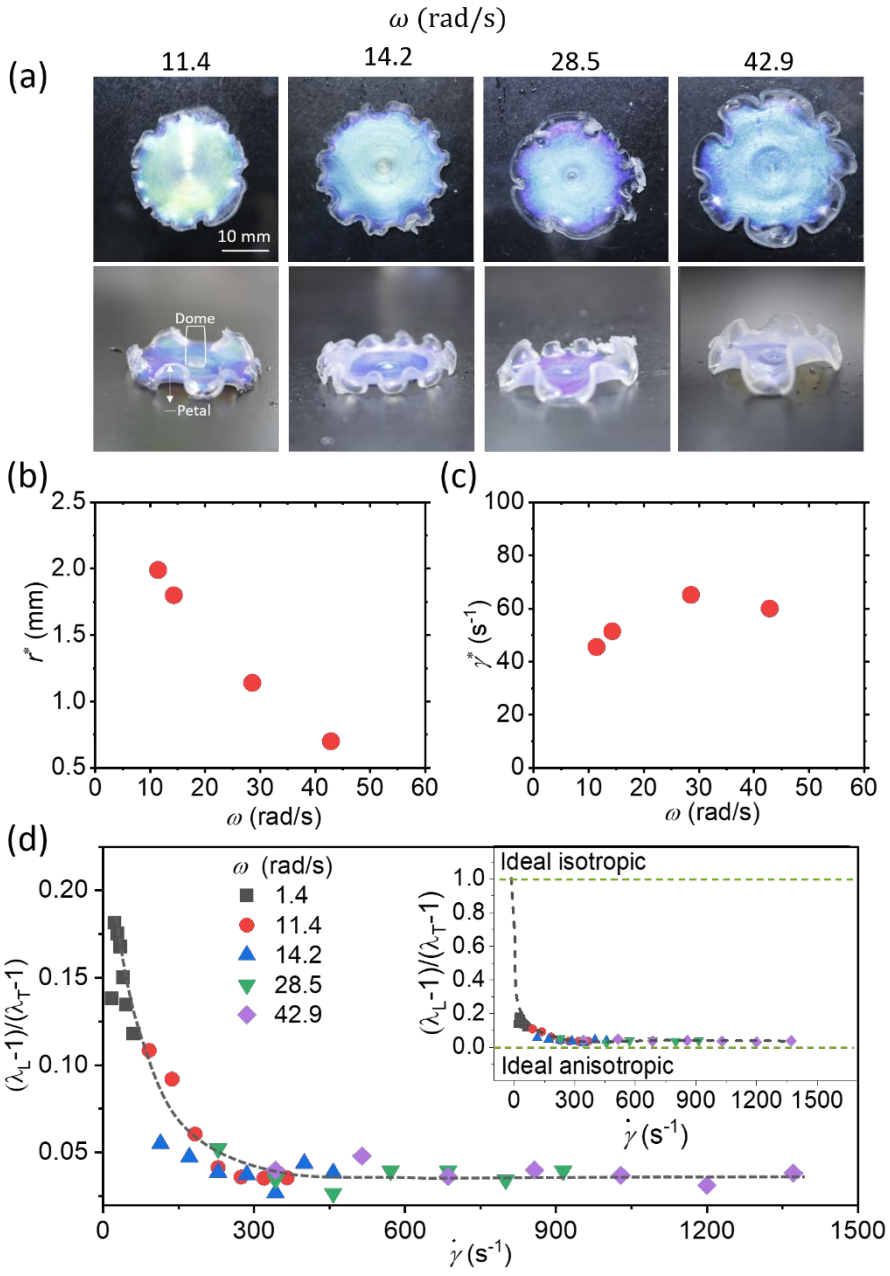

Figure 3. Gradient gel flowers fabricated under different angular speeds ω. There are three regions from center to edge: dome with less orientation, middle rings with well-aligned lamellar structure and edge petal with isotropic structure. (a) Photographs of gel flowers prepared at different angular speeds ω of 11.4, 14.2, 28.5 and 42.9 rad/s. The angular speed dependence of (b) radius of dome r^*, (c) critical shear rate calculated from $\omega r^*/t$. (d) The dependence of anisotropy parameters $(\lambda_L - 1)/(\lambda_T - 1)$

on shear rate $\dot{\gamma}$, in which the $(\lambda_L - 1)/(\lambda_T - 1)$ was calculated from the swelling behavior of gel at different position (inserts in Figure 2c) from water to 10 wt.% PEG solution. The two green dashed lines in the upper and lower parts of the inset figure are the ideal isotropic line $((\lambda_L - 1)/(\lambda_T - 1) = 1)$ and ideal anisotropic line $((\lambda_L - 1)/(\lambda_T - 1) = 0)$, respectively.

Relaxation of aligned lamellar bilayers domains. In addition to the shear rate, another important parameter controlling the alignment of lamellar bilayers is the lifetime of aligned lamellar bilayers domains in the precursor solution. The formation of aligned lamellar bilayers by shear flow in precursor solution is not stable and will lose the alignment with time by thermal fluctuation. In the above experiments, the alignment of lamellar bilayer was fixed by introducing a PAAm network via UV polymerization immediately after shear flow. To study the lifetime of the aligned lamellar bilayers, the effect of UV delayed time, which is the time interval between the flow cessation and UV polymerization, was studied on a hydrogel with ω of 11.4 rad/s^{-1}. Figure 4 shows the evolution of the anisotropy parameters $(\lambda_L - 1)/(\lambda_T - 1)$, calculated from position 1 (as indicated in Figure 2a) at different UV delayed time. The $(\lambda_L - 1)/(\lambda_T - 1)$ firstly keeps constant and then has a sharp increase as increasing the UV delayed time. The transition point occurs around 10 min, indicating that the relaxation of the aligned lamellar bilayer domains begins to occur after 10 min. Therefore, the lifetime of the perfect aligned lamellar bilayer structure is in the order of 10 min.

This relaxation time should be related to the domain size of the lamellar bilayer in the precursor solution. Next, we estimated the lamellar domain size of DGI bilayers based on the rotational diffusion theory.[22] The diffusion coefficient for rotational motion of a substance is $D_{rot} = \frac{1}{6\tau_{rot}}$, where τ_{rot} is the rotational relaxation time. The D_{rot} is related to the radius of substance as $r = \sqrt[3]{\frac{k_B T}{8\pi\eta D_{rot}}}$, where k_B T, η are the Boltzmann constant, absolute temperature and solvent viscosity (here is water), respectively. Here, τ_{rot} can be considered as the lifetime of perfect aligned lamellar bilayer structure formed by shear (10 min). Using the viscosity of water at 328.15 K (0.5065 mPa.s),[23] we have r = 7.5 μm.

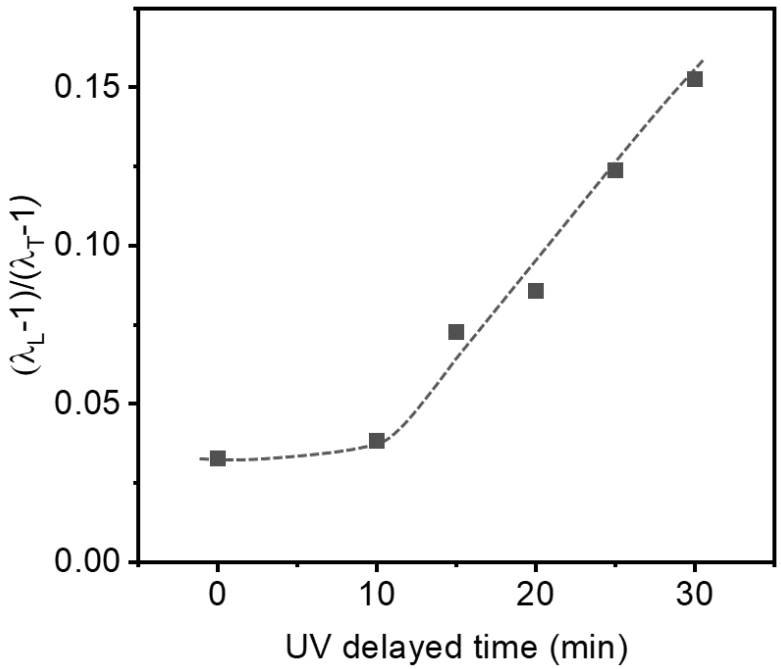

Figure 4. Effect of relaxation of the aligned bilayer in precursor solution on the gradient structure of gels. The UV delayed time dependence of anisotropy parameter at the position 1 in insert of Figure 2a.

Flower fades and reblooms. The hydrogel flower can fade and rebloom under external stimuli. Here we realize the fading and reblooming of hydrogel flower via water content change by deswelling of gel in 10 wt.% PEG aqueous solution and reswelling in pure water. When the photonic hydrogel flower was transferred from water to PEG solution, the osmotic pressure of PEG leads to the deswelling of the hydrogel. As a result, the gel is dehydrated to reach a new equilibrium state in PEG solution. The gel flower losses its color and decreases in size, which is named as fading, as shown in **Figure 5a** and **Movie. S1**. After bringing the hydrogel back to pure water, the transparent gel blooms and recovers to the original color and shape (**Figure 5b** and **Movie. S2**). The fading/reblooming behavior of the hydrogel flower is reversible. We demonstrated that at least 10 fading/reblooming could be repeated without obvious damping in responsiveness (**Figure S5**).

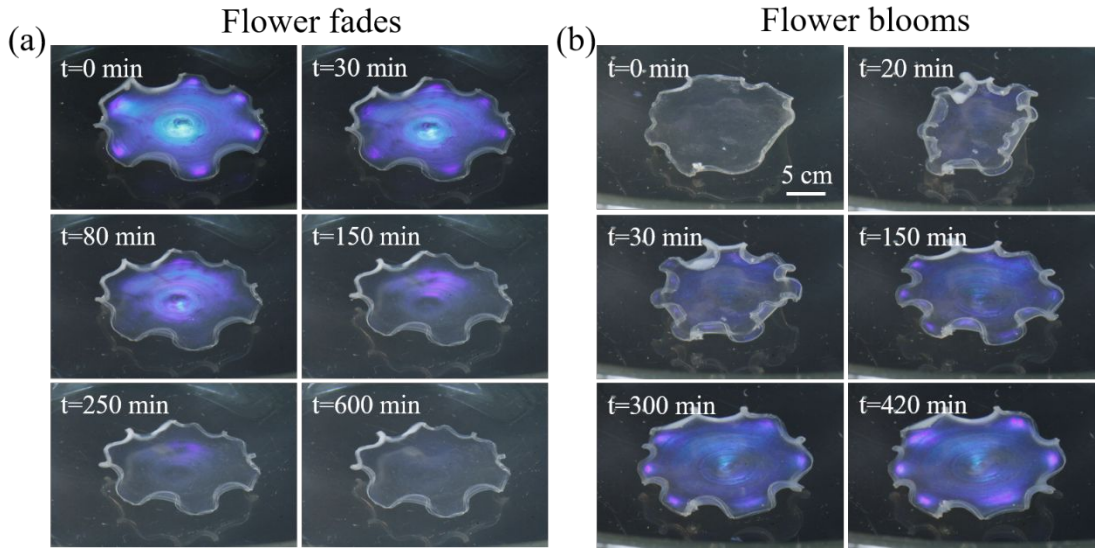

Figure 5. Solvent-triggered flower fades and blooms. (a) Photos showing that hydrogel flower fades in 10 wt.% PEG solution and (b) blooms in the water. Due to the gradient structure induced by the shear field, mismatch

of swelling/shrinking triggered the opening or fading of the photonic flower.

Conclusion We have developed a method to create superstructure in photonic PDGI/PAAm hydrogels through a customized rheometer equipped with a UV polymerization system. The distribution of shear field gives different orientation of lamellar bilayers, which causes swelling mismatch of the gel and consequently the formation of macroscopic hydrogels flower. The intrinsic shear parameter determining the shape of hydrogel flower and the lifetime of the aligned lamellar bilayers in the precursor solution were extracted. Furthermore, we also demonstrated that the hydrogel flower could reversibly fade and rebloom under external stimuli. This work provides a promising strategy to create superstructure in hydrogels.

Experiment

Gel preparation. The aqueous precursor solution consists of 0.10 M dodecyl glyceryl itaconate (DGI), 0.025 mol % sodium dodecyl sulfate relative to DGI, 2 M acrylamide (AAm), 2 mM N,N′-methylenebis(acrylamide) (MBAA) as a cross-linker, and 2 mM Irgacure 2959 as an initiator. The precursor solution was kept in a temperature-controlled water bath for ~5 h at 55 °C to dissolve monomeric DGI powders and stabilize lyotropic liquid crystalline phases of DGI. Then the precursor solution was loaded between two coaxially aligned parallel disk plates of a customized rheometer. The upper plate made from stainless steel has a

radius of 17.5 mm and the lower plate made of glass has a larger radius of 20 mm. The gap between these two plates was kept as 0.5 mm in this work. The shear flow was imposed by the rotation movement of the upper plate while the lower plate was fixed. The angular speed ω used in this work ranges from 1.4 to 42.9 s^{-1}. The shear rate gradient across the plate radius was formed as $\dot{\gamma} = \omega r/t$, to give a gradient anisotropic structure from centers. Where *t* is the gap distance and *r* is the radial distance from the center of the circular plates. The rotation of the upper plate was performed for 20 s. After the cessation of shear flow, the precursor solution was polymerized in argon atmosphere through a UV polymerization system equipped with the shear device (details see Figure S1 and Figure 1c). Then the polymerized gel was immersed into water for 1 week to reach swelling equilibrium.

Swelling measurement. The photonic disk gels equilibrated in water was cut into ten pieces from center to edge with a size of $L_0 \times W_0 \times T_0\, mm$, where the L_0 W_0 and T_0 are the length (5 mm), width (2 mm), and thickness, respectively (Inset in Figure 2c). Then the gel pieces were immersed in 10 wt% PEG solution (Mn = 20000 g/mol) and the gels shrunk to a size of $L_1 \times W_1 \times T_1\, mm$ after reaching equilibrium state. The size ratios are $\lambda_L = \frac{L_0}{L_1}$ for lateral direction and $\lambda_T = \frac{T_0}{T_1}$ for thickness direction. The size of the gels was measured by dial calipers. The anisotropy parameter was calculated as $(\lambda_L - 1)/(\lambda_T - 1)$ to represent the degree of orientation for lamellar structure from center to edge.

Small-Angle X-ray Scattering. The SAXS measurements of photonic gel from center to edge were performed at beamline BL40B2 of synchrotron radiation X-ray facility SPring-8 (JASRI, Hyogo, Japan). The X-ray wavelength was 0.15 nm, and a sample-to-detector distance was 4.13 m. Both the X- and Y-pixel size of the detector were 100 μm. The X-ray exposure time was 10 s. The back scattering 2D patterns were recorded on an imaging camera. The 2D image was converted to 1D data using Fit2D analysis software. From the q value of the first-order peak, interlamellar spacing, d, was calculated as $d = 2\pi/q$.

Acknowledgments

The authors thank Dr. K. Cui for precious advice and manuscript revision. The SAXS experiments were performed at the BL40B2 of SPring-8 with the approval of the Japan Synchrotron Radiation Institute (JASRI) (Proposal number: 2016A1254). This research was supported by JSPS KAKENHI Grant Numbers JP17H06144 and JP17H06376. J. P. G. acknowledges Institute for Chemical Reaction Design and Discovery (ICReDD) established by World Premier International Research Initiative (WPI), MEXT, Japan.

Reference

(1) Creton, C. *Macromolecules* **2017**, *50* (21), 8297–8316.

(2) Gong, J. P. *Soft Matter* **2010**, *6* (12), 2583–2590.

(3) Ye, Y. N.; Frauenlob, M.; Wang, L.; Tsuda, M.; Sun, T. L.; Cui, K.; Takahashi, R.; Zhang, H. J.; Nakajima, T.; Nonoyama, T. *Adv. Funct. Mater.* **2018**, 1801489.

(4) Sun, T. L.; Kurokawa, T.; Kuroda, S.; Ihsan, A. Bin; Akasaki, T.; Sato, K.; Nakajima, T.; Gong, J. P.; Haque, M. A.; Nakajima, T.; Gong, J. P. *Nat. Mater.* **2013**, *12* (10), 932–937.

(5) Hoffman, A. S. *Adv. Drug Deliv. Rev.* **2012**, *64*, 18–23.

(6) Seliktar, D. *Science (80-.).* **2012**, *336* (6085), 1124–1128.

(7) Lieber, R. L. *Skeletal muscle structure, function, and plasticity*; Lippincott Williams & Wilkins, 2002.

(8) Gao, H.; Ji, B.; Jäger, I. L.; Arzt, E.; Fratzl, P. *Proc. Natl. Acad. Sci.* **2003**, *100* (10), 5597–5600.

(9) Nalla, R. K.; Kinney, J. H.; Ritchie, R. O. *Nat. Mater.* **2003**, *2* (3), 164–168.

(10) Wegst, U. G. K.; Bai, H.; Saiz, E.; Tomsia, A. P.; Ritchie, R. O. *Nat. Mater.* **2015**, *14* (1), 23–36.

(11) Shtein, Z.; Shoseyov, O. *Proc. Natl. Acad. Sci.* **2017**, *114* (3), 428–429.

(12) Guido, N. J.; Wang, X.; Adalsteinsson, D.; McMillen, D.; Hasty, J.; Cantor, C. R.; Elston, T. C.; Collins, J. J. *Nature* **2006**, *439* (7078), 856–860.

(13) Takahashi, R.; Wu, Z. L.; Arifuzzaman, M.; Nonoyama, T.; Nakajima, T.; Kurokawa, T.; Gong, J. P. *Nat. Commun.* **2014**, *5* (1), 1–7.

(14) Chen, X.; Mayama, H.; Matsuo, G.; Torimoto, T.; Ohtani, B.; Tsujii, K. *J. Colloid Interface Sci.* **2007**, *305* (2), 308–314.

(15) Tsujii, K.; Hayakawa, M.; Onda, T.; Tanaka, T. *Macromolecules* **1997**, *30* (24), 7397–7402.

(16) Naitoh, K.; Ishii, Y.; Tsujii, K. *J. Phys. Chem.* **1991**, *95* (20), 7915–7918.

(17) Haque, M. A.; Kamita, G.; Kurokawa, T.; Tsujii, K.; Gong, J. P. *Adv. Mater.* **2010**, *22* (45), 5110–5114.

(18) De Kort, G. W.; Leoné, N.; Stellamanns, E.; Auhl, D.; Wilsens, C. H. R. M.; Rastogi, S. *Polymers (Basel)*. **2018**, *10* (9), 935.

(19) Krishnan, J. M.; Deshpande, A. P.; Kumar, P. B. S. *Rheology of complex fluids*; Springer, 2010.

(20) Li, X.; Kurokawa, T.; Takahashi, R.; Haque, M. A.; Yue, Y.; Nakajima, T.; Gong, J. P. *Macromolecules* **2015**.

(21) Haque, M. A.; Cui, K.; Ilyas, M.; Kurokawa, T.; Marcellan, A.; Brulet, A.; Takahashi, R.; Nakajima, T.; Gong, J. P. *Macromolecules* **2020**, *53* (12), 4711–4721.

(22) Ehrenberg, M.; Rigler, R. *Chem. Phys.* **1974**, *4* (3), 390–401.

(23) Kestin, J.; Sokolov, M.; Wakeham, W. A. *J. Phys. Chem. Ref. Data* **1978**, *7* (3), 941–948.